

GALAXY MERGERS AND THE MASS-METALLICITY RELATION: EVIDENCE FOR NUCLEAR METAL DILUTION AND FLATTENED GRADIENTS FROM NUMERICAL SIMULATIONS

DAVID S. N. RUPKE, LISA J. KEWLEY, & JOSHUA E. BARNES

Institute for Astronomy, University of Hawaii, 2680 Woodlawn Dr., Honolulu, HI 96822

Accepted by ApJL, 6 Jan 2010

ABSTRACT

Recent results comparing interacting galaxies to the mass-metallicity relation show that their nuclear oxygen abundances are unexpectedly low. We present analysis of N-body/SPH numerical simulations of equal-mass mergers that confirm the hypothesis that these underabundances are accounted for by radial inflow of low-metallicity gas from the outskirts of the two merging galaxies. The underabundances arise between first and second pericenter, and the simulated abundance dilution is in good agreement with observations. The simulations further predict that the radial metallicity gradients of the disk galaxies flatten shortly after first passage, due to radial mixing of gas. These predictions will be tested by future observations of the radial metallicity distributions in interacting galaxies.

Subject headings: galaxies: abundances — galaxies: evolution — galaxies: interactions — galaxies: ISM

1. INTRODUCTION

Galaxy interactions are major actors in the process of galaxy evolution. Because of this leading role, the impact of interactions on the chemical evolution of galaxies has become a subject of intense scrutiny. We know little about heavy elements in interacting galaxies, compared to our understanding of more isolated systems.

One place to look for signatures of chemical evolution is the mass-metallicity relation of galaxies (Lequeux et al. 1979; Rubin et al. 1984). Low-mass galaxies contain fewer heavy elements than high-mass galaxies, due to differing star formation histories combined with the action of gas inflows and outflows (Garnett 2002; Tremonti et al. 2004). In particular, star formation enriches the interstellar medium via nucleosynthesis; gas inflows of relatively metal-poor gas, either from outside the galaxy or interior to the galaxy, can change the galaxy's metal distribution; while outflows prevent further enrichment by blowing out recently produced metals (Edmunds 1990; Edmunds & Greenhow 1995; Köppen & Edmunds 1999; Dalcanton 2007).

Recent studies reveal that galaxies involved in major interactions fall below this fundamental relation. In other words, the centers of interacting galaxies are underabundant compared to galaxies of similar mass (Kewley et al. 2006; Rupke et al. 2008; Ellison et al. 2008; Michel-Dansac et al. 2008; Peeples et al. 2009). The physical model for these deviations from the $M - Z$ relation is attractively straightforward. If one or both of the progenitor galaxies is a spiral galaxy, radial abundance gradients exist in the merging galaxies (Zaritsky et al. 1994; van Zee et al. 1998), with lower abundances at larger galactocentric radius. During the merger, low-metallicity gas from the galaxy outskirts is torqued into the high-metallicity galaxy center (Mihos & Hernquist 1996; Barnes & Hernquist 1996), resulting in gas with a lower average abundance.

This gas redistribution should also result in a change in the gas metallicity profile across the entire disk.

Thus, radial metallicity gradients in mergers will differ from those in normal spirals. Barred galaxies, which are undergoing radial redistribution of gas due to bar-induced gas motions, indeed show evidence of either shallower gradients than are typical of unbarred spirals (Vila-Costas & Edmunds 1992; Zaritsky et al. 1994; Dutil & Roy 1999) or flattened oxygen gradients outside the corotation radius (Martin & Roy 1995; Roy & Walsh 1997). They also shower lower central metallicity than galaxies of similar morphological type and luminosity (Dutil & Roy 1999), as is observed in mergers. Friedli et al. (1994) model this behavior and demonstrate that the metal gradient changes are due to gas redistribution by the bar potential. A brief mention of metal redistribution in paired galaxies in the context of a coarse-grained cosmological simulation is also made in Perez et al. (2006). However, the idea of radial gas profile changes has not been quantitatively explored using detailed numerical simulations in the context of strongly interacting galaxies, which are undergoing even more violent gas redistributions than barred spirals.

We here analyze N-body / smoothed-particle hydrodynamics (SPH) simulations of galaxy mergers to quantitatively study metal redistribution due to merger-induced gas motions. We wish to explore nuclear metallicity and radial metal gradients as a function of time in the context of a merger of equal-mass spirals. This particular scenario is relevant to the formation of ultraluminous infrared galaxies (ULIRGs) and QSOs, which are thought to arise from such a merger (Sanders et al. 1988; Veilleux et al. 2002). §2 introduces our simulations and analysis. In §§3–4 we present and discuss our results, and we summarize in §5.

2. SIMULATIONS AND ANALYSIS

Our starting point is eight N-body/SPH simulations of close-passage, equal-mass disk galaxy mergers. These simulations use the setup described in in §3.1 and Appendix A of Barnes (2004), except that ours exclude star formation. In brief, 87040 particles (24576 gas) were used. Gas mass fractions (as a fraction of the stellar+gas

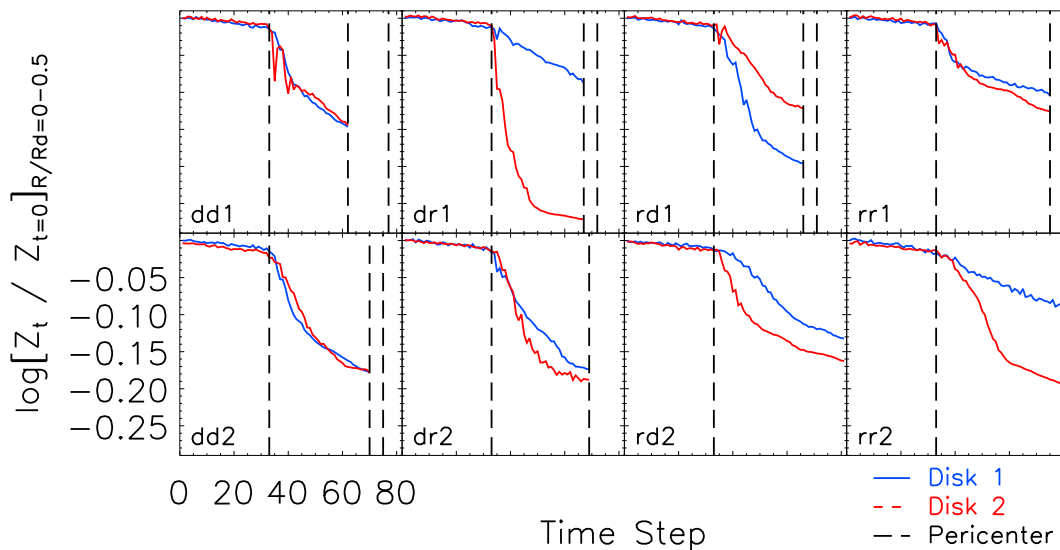


FIG. 1.— Change in nuclear ($R/R_d < 0.5$) metallicity as a function of time. The metallicity is expressed in terms of Z , the mass ratio of an element to that of hydrogen. Strong evolution is observed between first and second pericenter, of typical magnitude 0.2 dex. The change in nuclear abundance is not strongly dependent on geometry, and correlates very well with the amount of gas inflow (Figure 2). Vertical dashed lines locate the time of each pericenter, and data beyond the second pericenter is not plotted because of intermingling of the two gas disks.

mass) were set at 12.5%, and the gas was distributed in the same way as the stellar disk: in an exponential disk with constant scale height equal to 6% of the disk scale length. A cuspy stellar bulge was included, with a mass $1/3$ that of the stellar disk.

The mergers were distributed evenly across the phase space of initial geometries, with 2 simulations each from direct+direct, direct+retrograde, retrograde+direct, and retrograde+retrograde. (Direct and retrograde refer to the direction of rotation of each disk with respect to the encounter orbit.) For each of these four combinations, we chose two fairly close encounters with initial pericenters around $R_{\text{pericenter}}/R_{\text{disk}} \sim 1$ and 2. Each simulation is labeled self-evidently (e.g., dd1 = direct–direct for disks 1 and 2, respectively, and $R_p/R_d \sim 1$). Exact values of R_{peri} , inclination, and the direction of the line of nodes were chosen randomly within the constraints of direct/retrograde.

With this set of conditions, we are not probing all of parameter space, but focusing on the case of a strong interaction between two present-day spirals of roughly equal mass. This is most relevant to the formation of ULIRGs and QSOs in the local universe (§1). Future work will focus on a wider range of parameter space.

To get a sense of length scales, we note that for the best-fit simulation to NGC 4676 considered in Barnes (2004), the linear scale was such that $R_d = 3$ kpc. This is comparable to the disk scale lengths of spirals, which average several kpc (Zaritsky et al. 1994).

We calculate quantities of interest for each disk, assuming that little mass transfer occurs from disk to disk. This is a valid assumption up to the second pericenter, when the disks begin to overlap appreciably. We thus constrain our analysis to before second pericenter.

We include chemical evolution in our analysis by assigning metallicities to the gas particles at the begin-

ning of the simulation using the average gradient (per disk scale length) measured by Zaritsky et al. (1994), -0.2 dex/ R_d . The dispersion in the Zaritsky et al. (1994) sample is 0.1 dex/ R_d . We also add to each particle a normally-distributed random component to the metallicity, with $\sigma = 0.1$ dex and mean of 0. We then fix the metallicity of each gas particle for the duration of the simulation and follow the gas particles with time.

We neglect enrichment from star formation, since we are focused on spiral galaxies in the nearby universe. Gas mass fractions are small in local, massive spirals ($\sim 10\%$; Kannappan 2004), so further enrichment will be small compared to that from previous generations of stars. (See §4 for further discussion.) We are beginning a study of simulations involving star formation (Springel & Hernquist 2003), which will be considered in future work.

To study the radial metallicity distribution, at each time step we average azimuthally in radial bins of size $0.1 R_d$. We compute the gradient using a linear fit to the average metallicity in each bin, weighting each radius equally and fitting from 0 to $5 R_d$. (If, as mentioned above, $R_d \sim 3$ kpc for the progenitor disks, then the upper radius considered is ~ 15 kpc). This is comparable to the gradient measurement an observer makes, with H II regions distributed roughly evenly in radial space.

3. RESULTS

The finding that motivated this study was the observation that interacting galaxies have suppressed nuclear metallicities compared to isolated galaxies of similar luminosity or mass (Kewley et al. 2006; Ellison et al. 2008; Rupke et al. 2008; Michel-Dansac et al. 2008; Peebles et al. 2009). In Figure 1, we show that this effect is present in the simulations. The metallicity is unchanged prior to first pericenter, but it drops dramati-

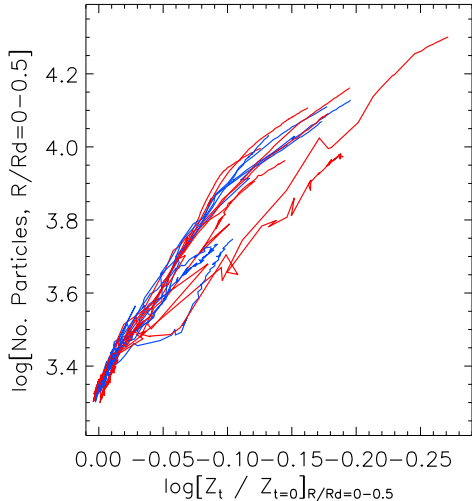


FIG. 2.— Change in nuclear metallicity vs. number of gas particles within the same radius. Each track represents the time evolution of a particular disk (disk 1 in blue, disk 2 in red) for each simulation, from lower left to upper right. The strong correlation is unambiguous, demonstrating that the underabundance is caused by gas inflow.

cally after first passage. By second pericenter, the change in metallicity ranges from -0.1 dex to -0.3 dex, with an average of -0.2 dex. The effect is more dramatic if the initial gradient is steeper (see below). The change in nuclear metallicity is correlated with the amount of gas inflow to the central region (Figure 2), confirming the suggestion that it is due to the dilution of the central metallicity as lower-metallicity gas flows inward from the outskirts of the system.

Turning to the metallicity profile of the entire disk, we show in Figure 3 the radial metallicity profile vs. time. Strong evolution from the initial distribution is evident, with the disks converging to a shallow or flat distribution over several disk scale lengths between first and second pericenter. The profile is not at all times characterized perfectly by a straight line, and tends toward a steeper negative slope in the innermost regions.

Radial mixing also results in an increase in the dispersion of the metallicity of the gas particles. From an initial dispersion of 0.1 dex, the dispersion within $R/R_d < 0.5$ rises to a value of 0.15 to 0.25 dex at second pericenter. At larger radii, the change in dispersion is more dramatic: it jumps to a typical value of 0.2 – 0.25 right after first pericenter. This dispersion contributes to the jagged radial profiles at large radius and late times, which is also caused by small number statistics and discrete tidal structures.

Accompanying the decrease in nuclear metallicity (Figure 1) is an increase in metallicity beyond $R \sim 3 R_d$ (Figure 3). This results from tidal tails that have spun out from the interiors of the progenitor disks, carrying small amounts of more metal-enriched gas from the galaxy centers into the outskirts. This removal of metals is insignificant compared to the effect of radial inflow, in terms of the gas mass involved. Thus, the gas removal from the inner regions has no effect on the central metallicity. However, because of the relatively small gas mass at large radii, mixing of small amounts of more enriched

gas easily raises the gas metallicity in these regions.

To quantify the profile evolution, in Figure 4 we show the gradient as a function of time. We observe the following about the gradient: (1) it changes little before first passage; (2) it drops precipitously after first passage (by 0.1 to 0.15 dex/ R_{disk}); and (3) it experiences mild evolution after this first drop. The degree of change varies little with encounter geometry, but there is evidence that the dd1/2 models experience the most change, while the rr1/2 models experience the least.

How does the change in gradient relate to the change in nuclear metallicity, which is more easily measured? Our models predict that, in the case of a major merger, the two quantities are loosely correlated (Figure 5). However, the change in gradient proceeds more quickly than the change in nuclear metallicity, with the latter being most dramatic after the gradient has already flattened substantially. This is due to the large gas mass of the central region, which requires significant inflow for its metallicity to be strongly affected.

In Figure 5, we demonstrate that the flattening of the gradient is not a strong function of the initial gradient, by comparing initial gradients of -0.2 and -0.4 dex/ R_d , which correspond to the average and the steepest gradients observed by Zaritsky et al. (1994). The range of gradients near second pericenter is 0 to -0.1 dex and -0.05 to -0.2 dex, respectively. However, the change in nuclear metallicity can be much higher if the initial gradient is steeper. More precisely, the final change in nuclear metallicity (in dex) is roughly equal to the initial gradient (in dex/ R_d).

4. COMPARISON TO OBSERVATIONS

Our results on nuclear underabundances compare favorably with observations. Previous work on a wide variety of interacting systems shows that underabundances are typically 0.1 – 0.3 dex (Kewley et al. 2006; Rupke et al. 2008; Ellison et al. 2008; Michel-Dansac et al. 2008), although higher underabundances exist in some massive, blue systems (Peeples et al. 2009). Our simulated offsets are consistent with most of these results, though an unknown fraction of the observed interacting systems represent weak or minor mergers. However, we cannot explain the strongest deviations of 0.6 – 0.8 dex (Peeples et al. 2009) unless the initial gradients are steeper than those measured by Zaritsky et al. (1994) or the progenitors of these interacting systems were already underenriched due to lack of previous star formation (consistent with their blue colors).

The present work is most applicable to mergers of equal-mass galaxies; the only systems that we are sure meet this criteria are ULIRGs. The metallicity offsets in these systems average 0.1 dex and range up to 0.3 dex (Rupke et al. 2008)¹. Again, these results are in excellent agreement with the simulations, especially if we assume either that the initial gradients were somewhat shallower than predicted by Zaritsky et al. (1994) or that there has been modest re-enrichment due to star formation.

¹ These numbers are smaller than presented in Rupke et al. (2008), and result from an updated analysis made possible by a recalibrated mass-metallicity relation using the $[\text{N II}]/[\text{O II}]$ metallicity diagnostic (Kewley & Ellison 2008). This diagnostic is the most robust strong-line diagnostic (Kewley & Dopita 2002).

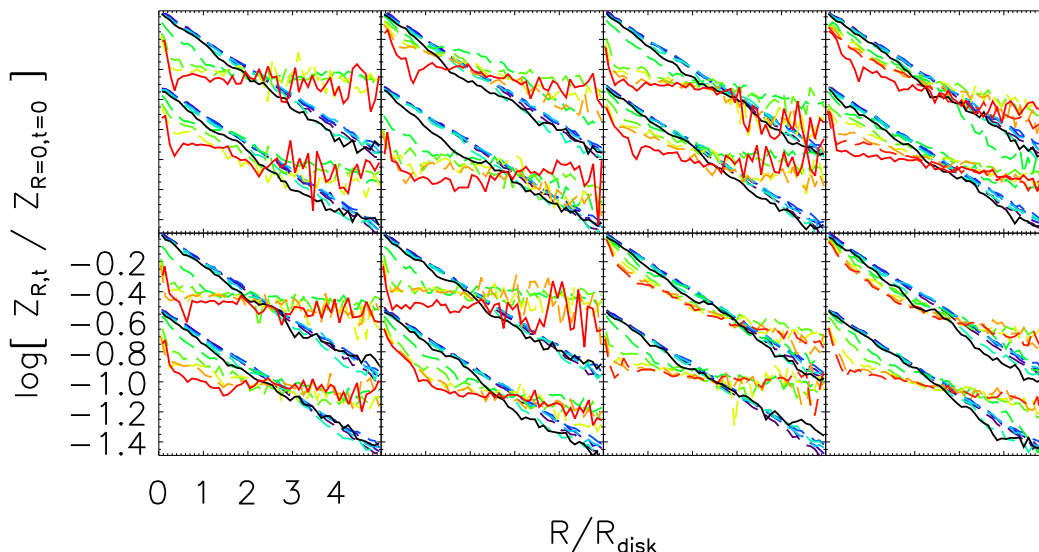


FIG. 3.— Radial metallicity profile at up to 10 time steps prior to second pericenter or the end of the simulation, whichever comes first. Blue (orange) dashed lines indicates early (late) times. The profile at first (second) pericenter is shown as a black (red) solid line. The profile for disk 2 is offset by -0.5 dex for clarity. Strong evolution toward a shallow or flat metallicity profile is evident between first and second pericenter.

There is no published data on the metallicity gradients of interacting systems. A study of weakly interacting spirals found no difference in metallicity gradient compared to isolated spirals (Márquez et al. 2003), but the $[\text{N II}]/\text{H}\alpha$ metallicity diagnostics used in this study have significant uncertainties (Kewley & Dopita 2002). We have begun a program to observe the gradients in strongly interacting galaxies, to understand how the metal redistribution occurs over the course of a merger and to compare to simulations.

It is clear that any significant galaxy-galaxy interaction will result in some change in the metallicity distribution of the galaxies involved. These effects may be important when interpreting the evolution of the mass-metallicity relation. At higher redshifts, when the merger and interaction rates were higher than at present (e.g., Kartaltepe et al. 2007), the dilution of nuclear abundances may be a more ubiquitous phenomenon. The effect will be especially significant if a population chosen to trace the evolution of the mass-metallicity relation consists of significant numbers of interacting systems. For instance, low-redshift Lyman Break Galaxy analogs show lower than expected metallicity and evidence of a major merger (Hoopes et al. 2007; Overzier et al. 2008). LBGs have been used to trace metallicity evolution at high redshift (Erb et al. 2006). However, higher redshift galaxies also have higher gas mass fractions, while our simulations assume a low gas mass fraction. Further work over a larger range of initial conditions is needed.

One caveat to our results is the presence of ongoing star formation, which we have ignored. Early in the merger, this star formation occurs across the disk of the galaxy, and hence is unlikely to change our conclusions about gradients. Late in the merger, star formation is heavily concentrated toward the galactic center, and can raise the heavy element content in these regions.

The magnitude of this effect depends on the initial

metallicity and the fraction of the remaining gas that is consumed in star formation. Consider two spirals with initial nuclear metallicities of Z_{\odot} and a true oxygen yield of 0.005 (Tremonti et al. 2004, reduced by a factor of two to account for their high metallicity calibration). Since a significant amount of gas remains at the late stages of a merger (Sanders et al. 1991), we assume that not more than half of the gas has been consumed prior to coalescence (more than this, and the initial gas mass fractions will have been unreasonably high). In the closed box model (Talbot & Arnett 1971), if 50% of the total gas mass is consumed in a solar-metallicity system, the metallicity will rise by at most 70%, or 0.2 dex. In this extreme scenario, enrichment by star formation could wipe out the nuclear metallicity underabundance predicted by our simulations, and may affect the gradient as well, depending on where the star formation occurred. However, comparison to the data shows that ongoing enrichment is small up to the ULIRG phase, since underabundances at the 0.1 – 0.3 dex level (or higher) are still observed in local interacting systems. This in turn implies that either we have assumed too much gas consumption in this example calculation (i.e., that the “extreme” case is not valid), or that outflows (which are ubiquitous in these systems; Rupke et al. 2005) have expelled metals produced in ongoing star formation, preventing further enrichment.

Either way, our simulation results appear robust to ongoing star formation. However, more sophisticated simulations involving both star formation and metal redistribution by supernovae and outflows will be required to confirm this. We are beginning to analyze numerical simulations of merging galaxies that include a prescription for chemical evolution due to star formation and stellar feedback (Springel & Hernquist 2003), especially to understand mergers at higher redshift with large gas mass fractions.

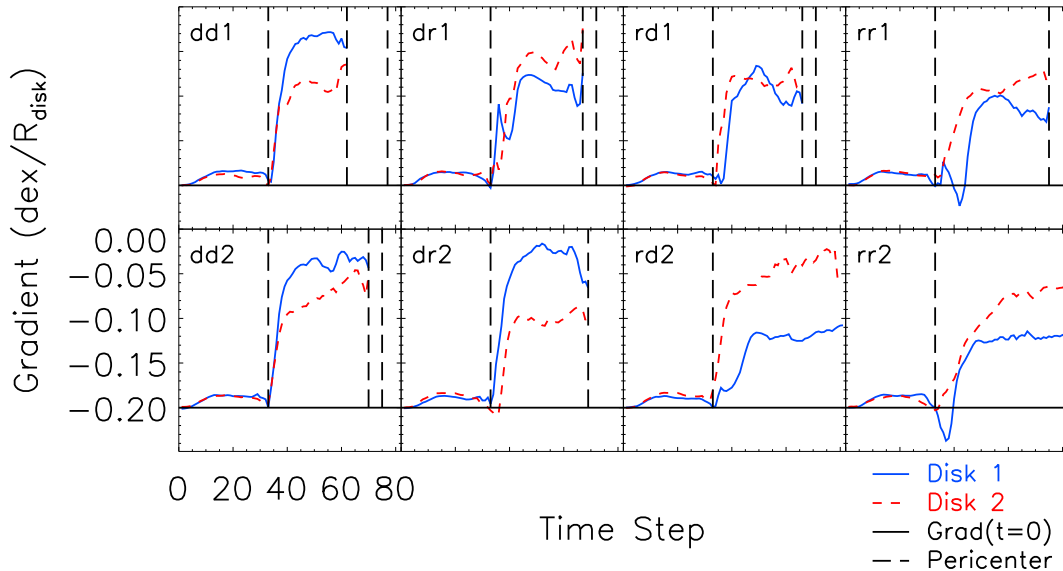


FIG. 4.— Radial metallicity gradient as a function of time. As suggested by Figure 3, the gradient abruptly turns shallow or flattens after first pericenter. The effect depends mildly on geometry, with retrograde+retrograde mergers showing the least effect.

5. SUMMARY AND PROSPECTS

We have presented numerical simulations that confirm that nuclear metallicity underabundances observed in interacting disk galaxies are due to merger-driven inflow of low-metallicity gas from the outskirts of the progenitor disks. The magnitude of the effect is in agreement with what is observed (~ 0.2 dex; Kewley et al. 2006; Rupke et al. 2008; Ellison et al. 2008; Michel-Dansac et al. 2008; Peeples et al. 2009). The nuclear metallicity drop traces closely the amount of merger-driven inflow, and is accompanied by an increase in the dispersion of gas cloud metallicities at a given radius. The metallicity drop and increase in dispersion occur predominantly between first and second pericenter.

Also evident between first and second pericenter is a dramatic flattening of the initial radial metallicity gradient. This flattening reflects the effects of gas redistribution over the galaxy disks. Such gradient changes will be observable in studies of H II region metallicities in strongly interacting systems. By comparing to detailed simulations, the distributions of gas-phase metallicities are certain to provide another way to constrain the evo-

lutionary state of interacting systems. In particular, they are very sensitive to the gas motions that occur within the system.

Our results apply primarily to local examples of major mergers of spiral galaxies. Analysis of simulations including more sophisticated chemical evolution prescriptions is currently underway, especially to probe a wider range of merger initial conditions (including mass ratio and gas mass fraction). It is important to understand the effect this could have on the determination of cosmic metallicity evolution, since galaxy mergers and interactions were more common at high redshift. Samples of high redshift galaxies that are dominated by interacting systems may bias metallicity determinations to low metallicities, compared to samples at low redshift dominated by isolated systems. Future work will explore this effect.

The authors thank the referee for a helpful report, and Fabio Bresolin for commenting on the manuscript. DSNR and LJK are funded by NSF CAREER grant AST07-48559.

REFERENCES

- Barnes, J. E. 2004, MNRAS, 350, 798, arXiv:astro-ph/0402248
 Barnes, J. E., & Hernquist, L. 1996, ApJ, 471, 115
 Dalcanton, J. J. 2007, ApJ, 658, 941, arXiv:astro-ph/0608590
 Dutil, Y., & Roy, J. 1999, ApJ, 516, 62
 Edmunds, M. G. 1990, MNRAS, 246, 678
 Edmunds, M. G., & Greenhow, R. M. 1995, MNRAS, 272, 241
 Ellison, S. L., Patton, D. R., Simard, L., & McConnell, A. W. 2008, AJ, 135, 1877, arXiv:0803.0161
 Erb, D. K., Shapley, A. E., Pettini, M., Steidel, C. C., Reddy, N. A., & Adelberger, K. L. 2006, ApJ, 644, 813, arXiv:astro-ph/0602473
 Friedli, D., Benz, W., & Kennicutt, R. 1994, ApJ, 430, L105
 Garnett, D. R. 2002, ApJ, 581, 1019, arXiv:astro-ph/0209012
 Hoopes, C. G. et al. 2007, ApJS, 173, 441, arXiv:astro-ph/0609415
 Kannappan, S. J. 2004, ApJ, 611, L89, arXiv:astro-ph/0405136
 Kartaltepe, J. S. et al. 2007, ApJS, 172, 320, 0705.2266
 Kewley, L. J., & Dopita, M. A. 2002, ApJS, 142, 35, arXiv:astro-ph/0206495
 Kewley, L. J., & Ellison, S. L. 2008, ApJ, 681, 1183, 0801.1849
 Kewley, L. J., Geller, M. J., & Barton, E. J. 2006, AJ, 131, 2004, arXiv:astro-ph/0511119
 Köppen, J., & Edmunds, M. G. 1999, MNRAS, 306, 317
 Lequeux, J., Peimbert, M., Rayo, J. F., Serrano, A., & Torres-Peimbert, S. 1979, A&A, 80, 155
 Márquez, I., Masegosa, J., Moles, M., Varela, J., Bettoni, D., & Galletta, G. 2003, Ap&SS, 284, 711
 Martin, P., & Roy, J. 1995, ApJ, 445, 161
 Michel-Dansac, L., Lambas, D. G., Alonso, M. S., & Tissera, P. 2008, MNRAS, 386, L82, 0802.3904

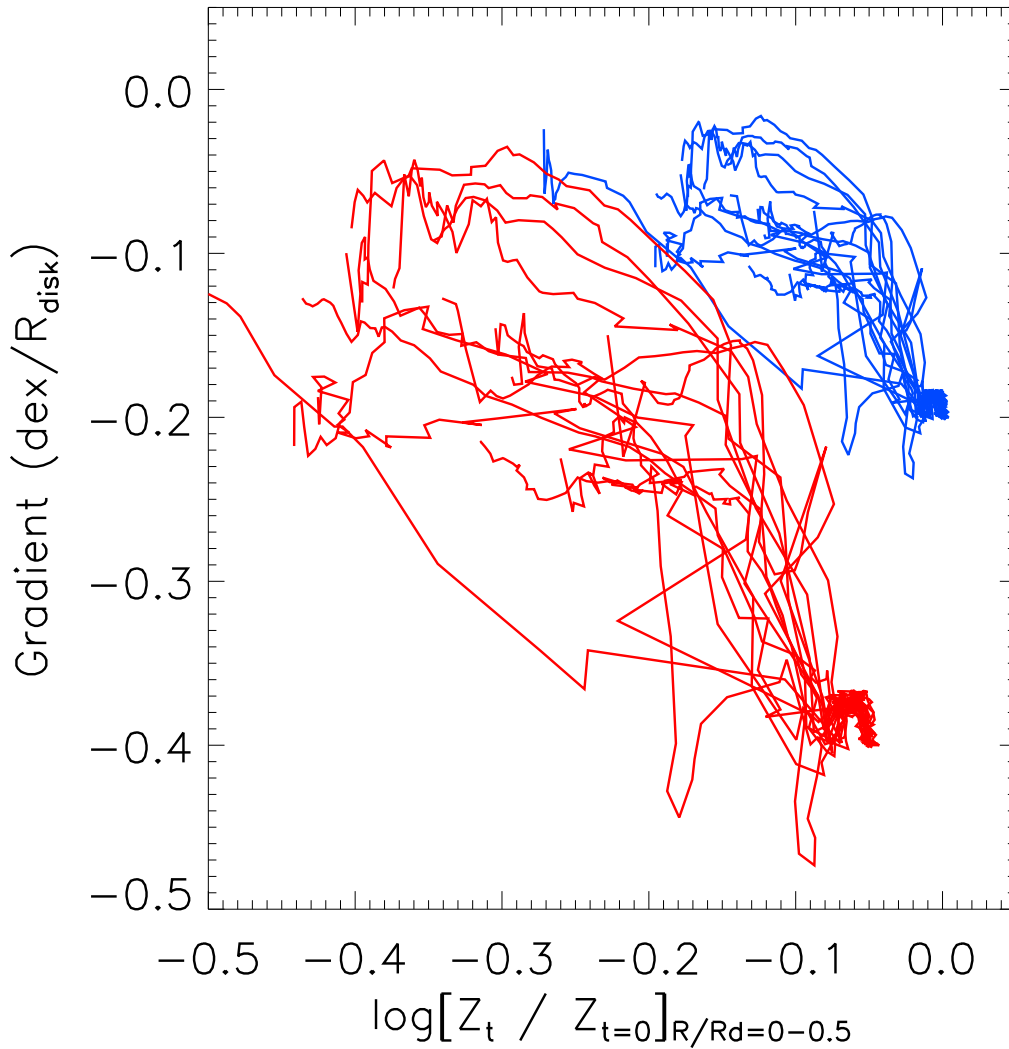


FIG. 5.— Change in nuclear metallicity vs. radial metallicity gradient. Each track represents the time evolution of a disk, from lower right to upper left. Blue (red) lines represent initial gradients of -0.2 (-0.4) dex/R_d . The two quantities are strongly linked, with some scatter. Steeper initial gradients result in lower nuclear metallicities, but still converge to shallow or flat gradients.

- Mihos, J. C., & Hernquist, L. 1996, *ApJ*, 464, 641, [arXiv:astro-ph/9512099](#)
- Overzier, R. A. et al. 2008, *ApJ*, 677, 37, 0709.3304
- Peeples, M. S., Pogge, R. W., & Stanek, K. Z. 2009, *ApJ*, 695, 259, 0809.0896
- Perez, M. J., Tissera, P. B., Scannapieco, C., Lambas, D. G., & de Rossi, M. E. 2006, *A&A*, 459, 361
- Roy, J., & Walsh, J. R. 1997, *MNRAS*, 288, 715, [arXiv:astro-ph/9705032](#)
- Rubin, V. C., Ford, Jr., W. K., & Whitmore, B. C. 1984, *ApJ*, 281, L21
- Rupke, D. S., Veilleux, S., & Sanders, D. B. 2005, *ApJS*, 160, 87, [arXiv:astro-ph/0506610](#)
- Rupke, D. S. N., Veilleux, S., & Baker, A. J. 2008, *ApJ*, 674, 172, 0708.1766
- Sanders, D. B., Scoville, N. Z., & Soifer, B. T. 1991, *ApJ*, 370, 158
- Sanders, D. B., Soifer, B. T., Elias, J. H., Madore, B. F., Matthews, K., Neugebauer, G., & Scoville, N. Z. 1988, *ApJ*, 325, 74
- Springel, V., & Hernquist, L. 2003, *MNRAS*, 339, 289, [arXiv:astro-ph/0206393](#)
- Talbot, Jr., R. J., & Arnett, W. D. 1971, *ApJ*, 170, 409
- Tremonti, C. A. et al. 2004, *ApJ*, 613, 898, [arXiv:astro-ph/0405537](#)
- van Zee, L., Salzer, J. J., Haynes, M. P., O'Donoghue, A. A., & Balonek, T. J. 1998, *AJ*, 116, 2805, [arXiv:astro-ph/9808315](#)
- Veilleux, S., Kim, D.-C., & Sanders, D. B. 2002, *ApJS*, 143, 315, [arXiv:astro-ph/0207401](#)
- Vila-Costas, M. B., & Edmunds, M. G. 1992, *MNRAS*, 259, 121
- Zaritsky, D., Kennicutt, Jr., R. C., & Huchra, J. P. 1994, *ApJ*, 420, 87